Catalysis Science & Technology

Oxidative Dehydrogenation of Propane over Transition Metal Sulfides Using Sulfur as an Alternative Oxidant

Journal:	*Catalysis Science & Technology*
Manuscript ID	CY-ART-05-2020-001039.R1
Article Type:	Paper
Date Submitted by the Author:	18-Aug-2020
Complete List of Authors:	Arinaga, Allison; Northwestern University Liu, Shanfu; Northwestern University Marks, Tobin; Northwestern University, Department of Chemistry

ARTICLE

Oxidative Dehydrogenation of Propane over Transition Metal Sulfides Using Sulfur as an Alternative Oxidant

Received 00th January 20xx,
Accepted 00th January 20xx

DOI: 10.1039/x0xx00000x

Allison M. Arinaga,[a] Shanfu Liu[a] and Tobin J. Marks [a*]

The use of alternative oxidants for the oxidative dehydrogenation of propane (ODHP) is a promising strategy to suppress the facile overoxidation to CO_x that occurs with O_2. Gaseous disulfur (S_2) represents a thermodynamically "softer" oxidant that has been underexplored and yet offers a potential route to more selective propylene formation. Here we describe a system for sulfur-ODHP (SODHP). We demonstrate that various metal sulfide catalysts generate unique reaction product distributions, and that propylene selectivities as high as 86% can be achieved at 450 - 550°C. For a group of 6 metal sulfide catalysts, apparent activation energies for propylene formation range from 72-134 kJ/mol and parallel the corresponding catalyst XPS sulfur binding energies, indicating that M-S bond strength plays a key role in SODHP activity. Kinetic data over a sulfided ZrO_2 catalyst indicate a rate law which is first-order in propane and zero-order in sulfur, suggesting that SODHP may occur via a mechanism analogous to the Mars van Krevelen cycle of traditional ODHP. The present results should motivate further studies of SODHP as a route to the selective and efficient oxidative production of propylene.

Introduction

Recent shifts from naphtha to shale gas feeds in cracking units have led to a renewed interest in "on-purpose" propylene production.[1] However, direct propane dehydrogenation is limited by thermodynamic constraints and catalyst deactivation due to extensive coking.[2] Oxidative dehydrogenation of propane with O_2 (ODHP) is an approach that has the potential to dramatically improve the efficiency of propylene production. This reaction is thermodynamically favorable owing to its exothermicity (Figure 1a), and coking is significantly suppressed under O_2.[3, 4] However, after years of research, achieving high propylene yields remains elusive due to overoxidation of the olefin product to CO and CO_2.[5] Investigations of novel approaches to ODHP are therefore needed to address this grand scientific challenge.

Recently elemental sulfur, in the form of S_2 vapor, has been implemented as a "soft" oxidant for the oxidative coupling of methane (OCM) to enhance ethylene selectivity by moderating the thermodynamic driving force towards over-oxidation.[6-8] S_2 is isoelectronic with O_2 and is the primary sulfur allotrope present in the gas phase above 700 °C (see Experimental Section for details on S_2 formation in this work).[9-11] This approach might also, in principle, be applicable to ODHP with S_2, as the Gibbs energy of reaction (ΔG_r) for total oxidation is far less severe with S_2 than for O_2 (Figure 1a). Furthermore, for methane, significant mechanistic differences are observed between S_2-OCM (SOCM) over metal sulfide catalysts versus traditional metal oxide-based OCM.[7, 8] These results raise the intriguing question of whether an S_2 oxidant and metal sulfide catalysts might display unique reactivity properties in an ODHP process as well.

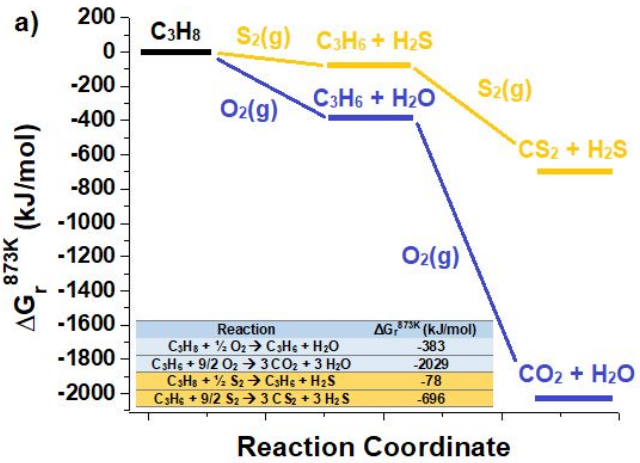

b) Commercial Claus Process:

$$2\ H_2S + 3\ O_2 \rightarrow 2\ SO_2 + 2\ H_2O$$
$$2\ H_2S + SO_2 \rightarrow 3\ S + 2\ H_2O$$

Figure 1. a) Reaction coordinate of the desired oxidative propane → propylene reaction and undesired total oxidation reaction, showing the Gibbs free energy of reaction for ODHP (blue) and SODHP (yellow) at 873 K. b) Claus process used to recover elemental sulfur from H_2S.

[a] *Department of Chemistry, Northwestern University, 2145 Sheridan Road, Evanston, IL 60208, USA*

† Electronic Supplementary Information (ESI) available: [details of any supplementary information available should be included here]. See DOI: 10.1039/x0xx00000x

Earth-abundant metal sulfides have proven to be promising, inexpensive catalysts for hydrocarbon transformations such as light alkane dehydrogenation.[12-18] Additionally, metal sulfides are tolerant to sulfur-containing compounds, which are present in most natural gas streams and which poison many noble metal and oxide-based catalyst alternatives.[19, 20] Shan et al. prepared sulfided metal oxide catalysts and reported that they exhibit higher activity and selectivity for isobutane dehydrogenation than the original oxide catalysts.[13-15] These authors argued that the increased selectivity reflects an electronic effect in which olefin desorption is facilitated on the sulfided catalyst surfaces. Nevertheless, these sulfided catalysts undergo rapid deactivation with time on stream due to loss of sulfur but can be regenerated by re-sulfiding the surface.

Peer-reviewed literature and patents have also described alkane ODH reactions promoted by sulfur, either in the form of H_2S added to the reactant stream or by using sulfate- or sulfide-based catalysts.[21-27] This sulfur addition is reported to enhance both ODH conversion and olefin selectivity. Several of these reports argue for *in-situ* formation of some active sulfur species such as S_2, produced via reaction of H_2S and O_2. Nevertheless, very little experimental data is available to support these models, and the relative roles of S_2 and O_2 oxidation are not easily differentiated.[21, 24, 27] Indeed, the limited reports in which elemental sulfur is proposed as an oxidant would be greatly strengthened by mechanistic data.

Overall, the prior literature on metal sulfide catalysts and sulfur promotion of light alkane activation suggests that a sulfur-ODHP (SODHP) process might be a promising route to acceptable propylene yields. Additionally, the H_2S byproduct formed from an SODHP process could be regenerated as elemental sulfur via the efficient industrial Claus process (Figure 1b).[28] In this contribution we describe a system for SODHP using elemental sulfur (S_2) as an oxidant and compare the catalytic results over six metal sulfide catalysts. The goal here is an exploratory study of the scope, fundamental chemistry, and mechanism of S_2 as an oxidant for ODHP. We report product selectivities, apparent activation energies (E_{app}), and reaction orders under differential conditions, leading to a plausible proposed reaction mechanism. These results demonstrate that sulfur vapor (S_2) can act as an effective oxidant for ODHP and that this novel SODHP process may be a promising new route to propylene production.

Experimental

Catalyst Preparation

In this study, bulk metal sulfides and sulfided metal oxides were employed as catalysts. Sulfided metal oxides will be denoted as S-M_xO_y, where M_xO_y is the metal oxide precursor. ZrO_2, TiO_2 (rutile), Cr_2O_3, Co_3O_4, MoS_2, and PdS powders were purchased from Sigma Aldrich. Prior to sulfidation or reaction, the materials were pressed into pellets, then crushed and sieved to achieve a mesh size of 180-300 μm. The metal sulfides MoS_2 and PdS were used as received without further pre-treatment. In order to ensure stable operating conditions under the sulfur-rich environment of the SODHP reaction, the metal oxides ZrO_2, TiO_2 (rutile), Cr_2O_3, and Co_3O_4 were pre-sulfided before the SODHP reaction by heating to 600 °C and holding for 6 h under a gas stream containing 0.28 wt% S_2 and 0.33 wt% H_2S. The sulfidation conditions were selected based on previous work on these and other similar sulfide catalysts for the oxidative coupling of methane with sulfur.[7]

Safety note: H_2S, a pretreatment gas and reaction product of this study, is lethal at concentrations of 750-1000 ppm. As such, the experimental setup should be contained in a well-ventilated area equipped with an H_2S monitor.

Catalyst Characterization

Powder X-ray diffraction (XRD) patterns of S-Co_3O_4 were acquired using a Scintag XDS2000 instrument, while all other catalyst XRD patterns were collected on a Rigaku Ultima Diffractometer. X-ray Photoelectron Spectroscopy (XPS) was carried out using a Thermo Scientific ESCALAB 250Xi instrument. An electron flood gun was applied prior to sample analysis. Peak fitting was performed using Thermo Avantage software. Physisorption measurements were performed with a Micromeritics 3Flex instrument, and surface areas were calculated using the Brunauer-Emmett-Teller (BET) method. Prior to measurements, metal sulfides and sulfided oxides were degassed at 120 °C for 6 h, while metal oxide precursors were degassed at 300 °C for 6 h. The BET surface areas of S-Co_3O_4 and PdS could not be determined due to loss of sulfur from the bulk under vacuum conditions.

Catalyst Evaluation

Catalytic reactions were carried out at atmospheric pressure between 450 and 550 °C in a custom flow reactor that has been described in detail previously.[6] Briefly, a sulfur evaporator, preheater furnace, and reactor furnace are contained within an insulated oven. The sulfur flow rate was adjusted by controlling the temperature of the sulfur evaporator (typically 180-220 °C). Prior to introduction into the reactor furnace, sulfur vapor was passed through the preheater furnace at 700 °C. At this temperature, S_2 is the predominant gaseous species compared to other gas-phase sulfur allotropes.[9-11] Gas flow rates were controlled using Brooks Model 5850E mass flow controllers.

The quartz reactor tube was charged with 100-200 mg of metal sulfide catalyst or oxide precursor before each reaction. The reactor was flushed with 120 sccm He while heating to reaction or sulfidation temperature. During the SODHP reaction, propane and sulfur were flowed for a minimum of 3 h. Products were analyzed by gas chromatography (Agilent 7890A) using flame ionization (FID) and thermal conductivity (TCD) detectors. The reported propane conversions (eq. 1) and product selectivities (eq. 2) were determined using the average of the last 90 min on stream and calculated on a molar basis. Here, C represents the concentration of a carbon-containing product and ν represents the number of carbon atoms in said product.

$$Conversion = \frac{C_3H_{8,\,in} - C_3H_{8,\,out}}{C_3H_{8,\,in}} \qquad (1)$$

$$Selectivity = \frac{\nu C_{product}}{\sum \nu C_{product}} \qquad (2)$$

Table 1. Structural characteristics and activity of catalysts after SODHP reaction. [a]

Catalyst	Phases detected by PXRD	XPS S2p$_{3/2}$ binding energy (eV)	BET surface area (m^2/g) [b]	Conversion (%)	Selectivity (%)	E_{app} (kJ/mol)
S-ZrO_2	ZrO_2	163.17	27	8.1	85.7	95.9
S-TiO_2	TiS_2, TiO_2	163.45	19	7.6	79.6	97.3
S-Cr_2O_3	Cr_2O_3	162.37	7	7.2	68.5	85.9
S-Co_3O_4	Co_3S_4, CoS	161.42	-	4.7	78.0	134
MoS_2	MoS_2	161.86	15	5.4	53.2	85.5
PdS	PdS	161.51	-	7.9	38.2	71.6

[a] Characterization and conversion/selectivity data acquired after SODHP at 550 °C for 3.5 h.

[b] Surface area of S-Co_3O_4 and PdS could not be measured due to loss of sulfur from the bulk under degas conditions.

Conversion and selectivity were calculated as an average of several time points to account for uncertainties in the GC peak areas of propane and other gases. Steady state catalyst performance was achieved prior to calculation of these values (see Figure S9 for stability of SODHP catalysts with time on stream). Additionally, weight hourly space velocity (WHSV) during the SODHP reaction was calculated by dividing the total mass flow rate of the feed gas (including propane, sulfur, and inerts) in grams/min by the total mass of catalyst loaded into the reactor in grams.

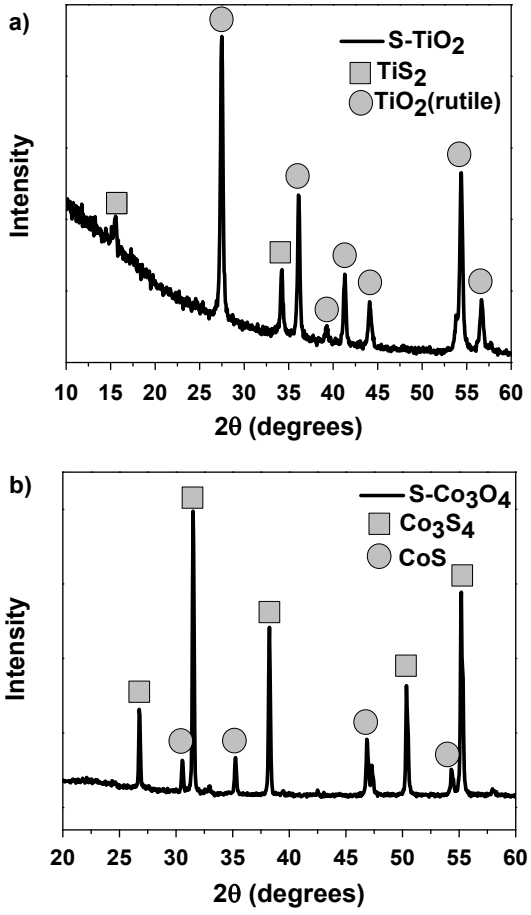

Figure 2. PXRD patterns of **a**) S-TiO_2 and **b**) S-Co_3O_4 after SODHP reaction at 550 °C.

Results and Discussion

Catalyst Characterization

The spent sulfided metal oxide catalysts were characterized in order to probe the effects of the sulfidation treatment and SODHP reaction conditions. The BET surface areas of the precursors and spent catalysts are summarized in Table 1 and Table S1. The surface areas of the spent catalysts are somewhat lower than those of the

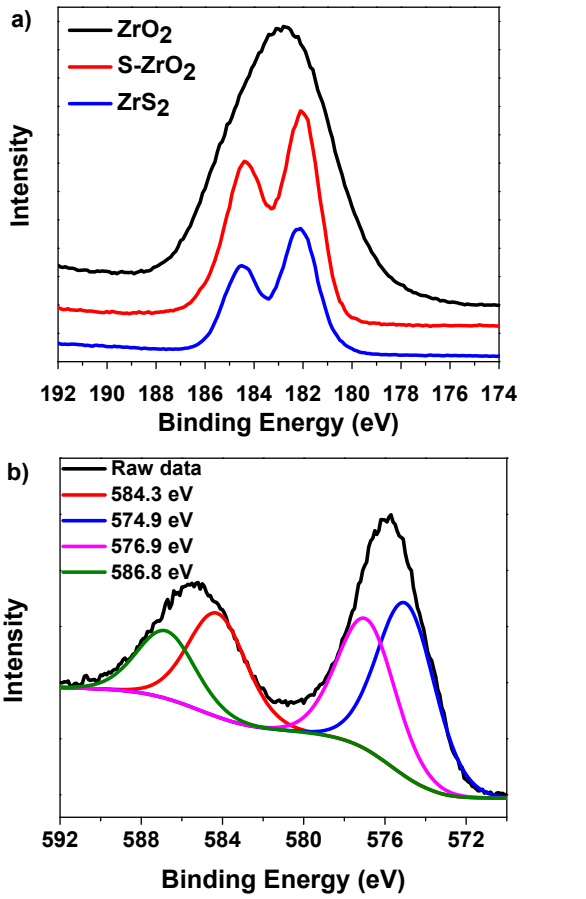

Figure 3. XPS spectra of **a**) the Zr3d region of the ZrO_2 precursor (black), S-ZrO_2 after sulfurization and SODHP at 550 °C (red), and a ZrS_2 standard (blue) and **b**) the Cr2p region of S-Cr_2O_3 after sulfurization and SODHP at 550 °C.

precursors, which is consistent with earlier SOCM studies and is expected upon transition from oxide to sulfide.[7, 29] The BET surface area of the MoS_2 catalyst is unchanged after the SODHP reaction. PXRD patterns of S-Co_3O_4 and S-TiO_2 reveal complete and partial transformation of the bulk into sulfides, respectively (Figure 2). Moreover, the S-ZrO_2 and S-Cr_2O_3 diffraction patterns exhibit no significant differences from those of the oxide precursors, indicating that any sulfide phase is either amorphous and/or present solely as a thin layer on the surface.

The XPS Zr3d spectrum of S-ZrO_2 contains a doublet with ionizations centered at 181.99 and 184.35 eV. These peaks match those of a ZrS_2 standard (Figure 3) as well as literature data. [30] The Cr2p spectrum of S-Cr_2O_3 contains a pair of spin-orbit doublets, which can be assigned to Cr_2O_3 and Cr_2S_3. The peak centered at 574.9 eV agrees well with the reported $Cr2p_{3/2}$ value for Cr_2S_3, while the peak at 576.9 eV falls into the reported range for Cr_2O_3.[31] Similarly, the Ti2p scan for S-TiO_2 displays four peaks corresponding to the spin-orbit doublets for TiS_2 and TiO_2 (Figure S2). These results suggest that S-ZrO_2 likely consists of a core-shell type structure with surface ZrS_2 and the ZrO_2 phase comprising the bulk. In contrast, S-Cr_2O_3 and S-TiO_2 contain both oxide and sulfide on the surface. While the presence of TiS_2 in the PXRD pattern of S-TiO_2 suggests some bulk oxide to sulfide conversion, S-Cr_2O_3 likely remains as Cr_2O_3 in the bulk. Similar structural trends were observed in previous studies on these catalysts.[7] Note that S-Co_3O_4 is completely sulfided into bulk Co_3S_4 and CoS according to the present PXRD data. The XPS spectrum reveals the presence of fully reduced Co^0 on the surface in addition to the expected Co^{II} and Co^{III} (Figure S3). Additionally, all the sulfided catalysts contain a spin-orbit doublet in the S2p region (see Table 1 and Figure S4), which further supports the formation of metal sulfides.[31]

The diffraction patterns of fresh and spent MoS_2 and PdS reveal that there are no phase changes following the SODHP reaction (Figure S5). However, spent PdS displays significantly sharper peaks compared to the fresh catalyst, suggesting increased crystallite dimensions/order. Additionally, the XPS spectra in the Mo3d and Pd3d regions display no observable change in metal oxidation state after the SODHP reaction (Figure S6), indicating that there is no significant loss of sulfur from the surface under catalytic reaction conditions.

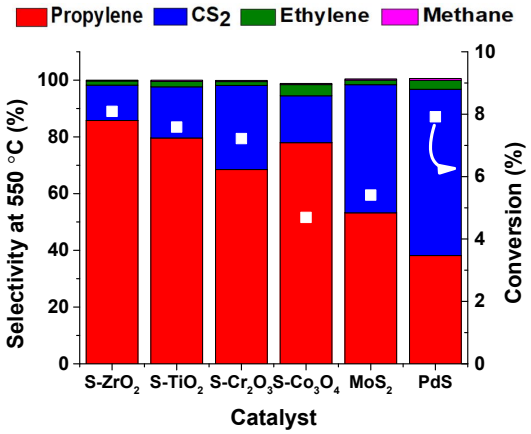

Figure 4. Product selectivity distributions (left axis) and propane conversions (right axis, white dots) for the 6 indicated catalysts during SODHP at 550 °C. Conditions: WHSV = 8.3 min^{-1}, propane/S_2 = 3.7.

Catalyst Evaluation

The six catalysts were investigated for SODHP over the 450-550 °C temperature range. A "blank reaction" using the same reactor filled with quartz sand was also performed to ensure there were no significant homogeneous gas phase reaction in this temperature range (Figure S10). All catalysts achieve steady-state conversion after 1-2 h on stream (Figure S9). Figure 4 compares the conversions and product distributions of the six catalysts. Propane conversion is significantly catalyst-dependent and varies from 4.7 to 8.1% at 550 °C. The major reaction products are propylene and CS_2. Less than 4% combined C2 and C1 products are detected at the highest temperature of 550°C, suggesting that C-C bond activation is a relatively minor pathway. The carbon balance exceeds 98% for all catalysts (Figure S11). In addition to carbon-containing products, H_2S is also detected in the product stream (see Table S3 for H_2S yields). The propylene selectivity varies widely, ranging from 86% over S-ZrO_2 to 38% over PdS. The range of propylene selectivities may be due to differences in activity for propane/propylene combustion or

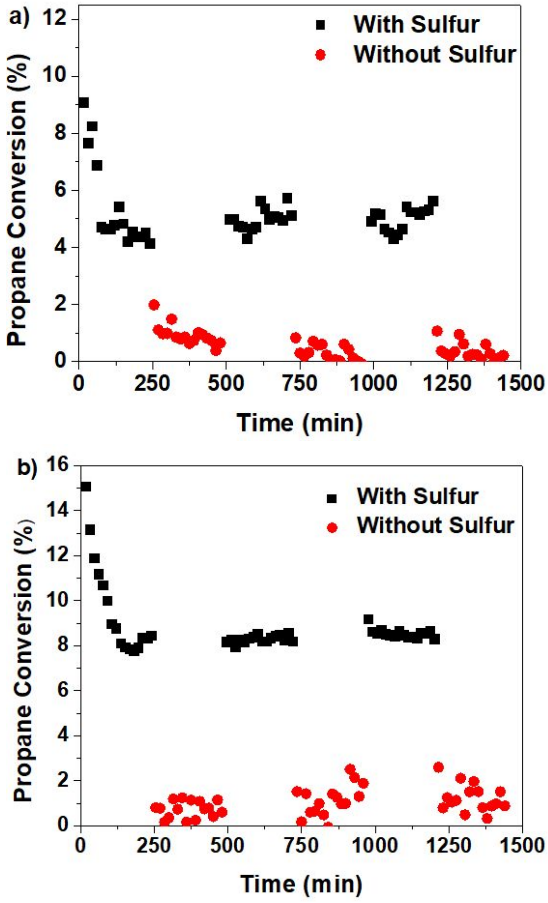

Figure 5. Propane conversion versus time on stream for **a**) MoS_2 and **b**) S-ZrO_2 in the presence (black squares) and absence (red dots) of S_2 in the reactant stream. In the absence of sulfur, the total flow rate was maintained using He as a balance gas. Conditions: WHSV = 8.3 min^{-1}, propane/S_2 = 3.7, T = 550°C.

desorption energetics of propylene from the surface. Selectivity also increases with temperature for all catalysts (see Figure S7). This trend is similar to that observed for traditional ODH and indicates that the activation energy for propylene overoxidation to CS_2 is lower than that for propane conversion to propene.[32] Thus, as the SODHP reaction is further studied in the future and reaction conditions are optimized, it may be preferable to operate between 500 – 550 °C, where high selectivity can be achieved without the intrusion of significant gas phase reactions.

Control experiments were next performed to examine the effect of sulfur (S_2) in the SODHP reaction. Without sulfur in the reactant feed, the propane conversion is significantly diminished over the sulfide catalysts. Figure 5 shows the results of experiments in which the flow is switched on and switched off while on stream over MoS_2 and S-ZrO_2. That is, the total gas flow rate is maintained constant while the flow is terminated using a balance flow of He. In a typical experiment, sulfur and propane flow over the catalyst. The propane conversion drops during the first 1-2 hours on stream before reaching steady state, which may be due to sintering, surface reconstruction, or the presence of active sites that are not regenerated. When the sulfur flow is terminated, the propane conversion falls significantly, but rapidly recovers to steady state levels upon reintroducing the sulfur flow. These results argue that there is little background non-oxidative dehydrogenation or thermal cracking of propane occurring under these conditions for both MoS_2 and S-ZrO_2, and that sulfur is an effective oxidant.

The relationship between propane conversion and product selectivity was also investigated by altering the contact time of the gas feed. As shown in Figure 6, higher propane conversions lead to reduced propylene and increased CS_2 selectivity over both S-ZrO_2 and MoS_2. The inverse relationship between conversion and propylene selectivity suggests that CS_2 is formed as a secondary product from propylene over-oxidation.[33] However, propylene selectivity does not reach 100% when extrapolated to zero conversion, indicating that some direct propane → CS_2 conversion is also operative.[33]

The trade-off between conversion and selectivity in ODHP is often severe.[34-38] For the present SODHP system, the severity of the trade-off is markedly catalyst-dependent. The propylene selectivity over MoS_2 drops considerably, from 49 to 22% at 2.6 and 10.9% conversion, respectively. In contrast, S-ZrO_2 displays a relatively moderate trade-off at low conversions, with the propylene selectivity only falling to 61% at the highest conversion tested (16%). Figure 7 shows the conversion-selectivity relationship for SODHP over S-ZrO_2 to those of ODHP over some well-studied transition metal oxide catalysts in the literature. Although the reaction conditions are not exactly identical, it can be seen that the propylene selectivity over S-ZrO_2 is comparable to the selectivities that have been reported for optimized traditional ODHP. In particular, the extent of the trade-off between conversion and selectivity over S-ZrO_2 rivals that of these literature examples. These results highlight that SODHP over metal sulfide catalysts can be an effective route to selective oxidative propylene production. Of course, SODHP is in its infancy, and further studies will likely yield more active and selective catalysts.

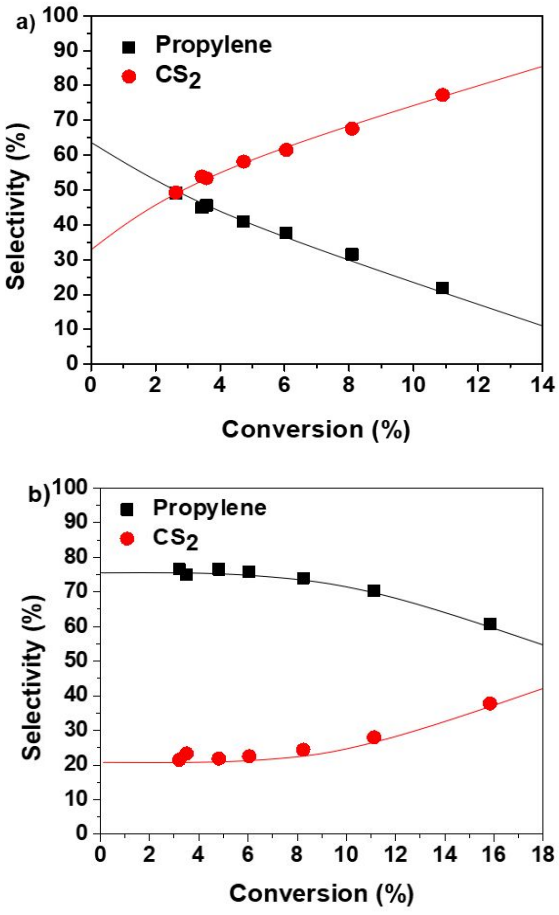

Figure 6. Propylene and CS_2 selectivity as a function of conversion during SODHP for a) MoS_2 and b) S-ZrO_2. Conditions: WHSV = 8.3 min^{-1}, propane/S_2 = 3.7, T = 510°C.

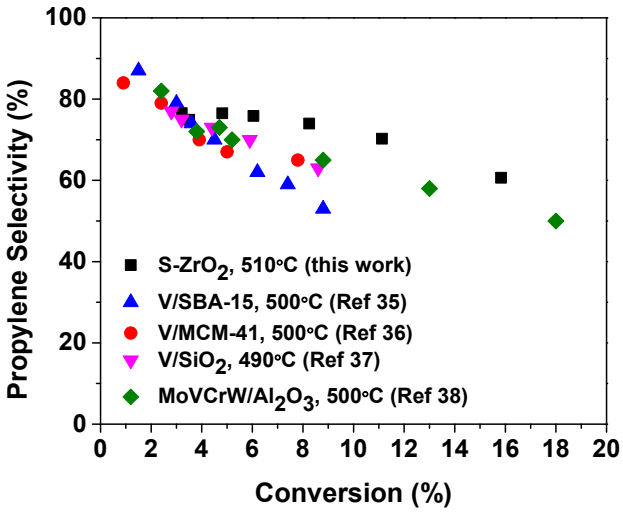

Figure 7. Propylene selectivity as a function of propane conversion over S-ZrO_2 (SODHP, this work) and some optimized transition metal oxide catalysts for ODHP with O_2. S-ZrO_2 conditions: WHSV = 8.3 min^{-1}, propane/S_2 = 3.7, T = 510°C.

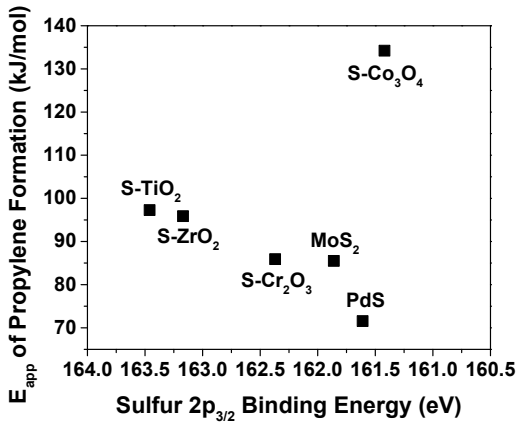

Figure 8. Apparent SODHP activation energy for propylene formation over the indicated six catalysts versus the XPS S$2p_{3/2}$ binding energy. Conditions: WHSV = 8.3 min^{-1}, propane/S_2 = 3.7, T = 470-550°C.

Mechanistic Characterization

Since the SODHP catalytic properties are strongly dependent on the metal sulfide identity, another question concerning this reaction is what intrinsic sulfide properties govern catalyst activity. Since neither the active site density nor the sulfide surface area could be accurately measured for these catalysts, reaction rates cannot easily be used to compare all six catalysts. Instead, the experimental E_{app} values for propylene formation were determined using the Arrhenius formalism and employed as activity descriptors. Note that E_{app} has frequently been used in the heterogeneous catalysis literature to describe catalyst activity and volcano trends.[39, 40] Table 1 summarizes the measured E_{app} value for each catalyst (see Table S2 for R^2 values from linear fit), and the Arrhenius plots can be found in Figure S12.

Several previous studies suggested that traditional ODHP over metal oxide catalysts proceeds via a Mars van Krevelen (MvK) mechanism, in which lattice oxygen species on the catalyst surface are consumed during alkane activation.[32, 38, 41-43] The resulting oxygen vacancies are then replenished by the gas phase O_2. For an MvK mechanism, the catalyst activity is typically determined by the reducibility of the catalyst or the metal-oxygen bond strength.[44] With this relationship in mind, we attempted to correlate the present SODHP catalytic activity with either of these parameters. Although the heat of formation has frequently been used as a rough estimate of the metal-oxygen or metal-sulfur bond strength,[45, 46] there is no obvious correlation between the bulk sulfide enthalpy of formation and the present E_{app} values. However, the heat of formation is a bulk property and does not necessarily describe surface properties.[47] In the absence of computed values, the sulfur XPS binding energy was selected as a surface specific metric of the metal-sulfur bond strength. Since the XPS binding energy represents the energy required to remove an inner electron, a larger sulfur binding energy suggests decreased electron density on the sulfur atoms/lower-lying bonding orbitals, and thus stronger M-S bonding.[48]

Figure 8 examines the correlation between the sulfur $2p_{3/2}$ binding energy and the E_{app} for SODHP. E_{app} decreases as the binding energy decreases (weaker M-S bonding). The exception is S-Co_3O_4, which has the largest barrier despite exhibiting the lowest sulfur binding energy. However, as the XPS data reveal (see Figure S3), this catalyst contains significant amounts of Co^0 on the surface. Note also that this Co^0 is not a reduction artifact arising from the argon sputtering since an ion beam was not applied before acquiring the XPS spectrum of this sample. The presence of Co^0 could indicate that the high E_{app} for S-Co_3O_4 may be due to structural differences versus the other metal sulfide catalysts. An alternative explanation is that we are observing an inverse "volcano" trend,[49] where beyond a certain sulfur binding energy the reaction kinetics change and E_{app} begins to increase. Note that the XPS sulfur binding energy does not necessarily scale linearly with actual M-S bond energy, meaning the slope visualized in Figure 8 may differ with DFT-calculated values.

Regarding the remaining five catalysts, a plausible rationalization for the observed trend is that weaker M-S bonds and more electron-rich/basic surface sulfur atoms facilitate hydrogen abstraction from propane. Similar trends have been reported previously for light alkane oxidation processes, including SOCM.[6, 50] To examine this hypothesis, the reaction orders of sulfur and propane were determined. As shown in Figure 9a, the rate of propane consumption over S-ZrO_2 is essentially invariant with the sulfur concentration, indicating a zero-order S_2 dependence (see SI Table S4 for the conversions and propylene selectivities). Propane: S_2 ratios greater than reaction stoichiometry were used here to ensure the observed zero-order dependence was not simply due to an overabundance of sulfur in the reactant stream. A similar result has been frequently described in the ODHP kinetics literature for O_2.[33, 41, 44] The propane order was next measured under excess sulfur. The natural logarithms of propane concentration and reaction rate display a linear relationship with a slope of 0.91 (see Figure 9b), suggesting first-order dependence in propane.

The sulfur order in the rate law was also measured for S-Co_3O_4 to ascertain whether there was a kinetic difference regarding the role of sulfur for this catalyst. Unlike S-ZrO_2, the reaction rate over S-Co_3O_4 increases with increasing sulfur concentration. Figure 9c shows that the relationship between the natural logarithms of sulfur concentration and rate yields a slope close to 0.5. This apparent half-order in S_2 for S-Co_3O_4 suggests mechanistically that there is a slow S_2 dissociation step during SODHP over this catalyst.

Considering the above results, the following mechanism is tentatively proposed for SODHP and summarized in Figure 10. The

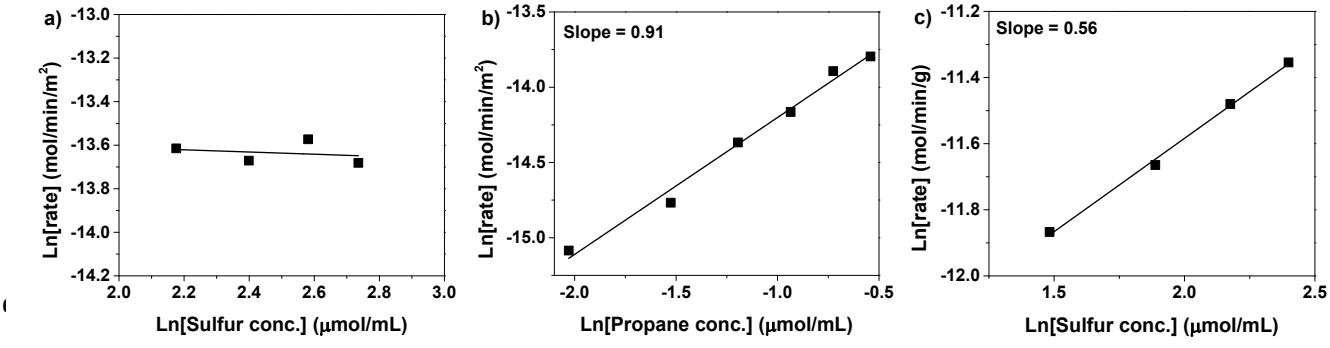

Figure 9. For SODHP, the natural logarithm of the a) sulfur concentration versus the natural logarithm of the reaction rate over S-ZrO_2 b) propane concentration versus the natural logarithm of the reaction rate on S-ZrO_2, and c) sulfur concentration versus the natural logarithm of the reaction rate on S-Co_3O_4. Conditions: WHSV = 8.3 min^{-1}, T = 510°C.

rate-determining step in SODHP over the present metal sulfide catalysts is propane C-H activation by a surface sulfur species, which leads to surface reduction. Hydrogen abstraction from the central carbon is typically rate-determining in oxide-mediated propane oxidations and is consistent with the observed first-order dependence on propane.[51, 52] A more active sulfur species would be expected when the metal-sulfur bonding is weaker and the sulfur atom is more electron dense, which in turn would lead to a lower E_{app}. The relationship illustrated in Figure 8 indeed follows this trend, as a lower sulfur binding energy is indicative of weaker metal-sulfur bonding. Following C-H activation, the formation of propylene and H_2S would then leave a sulfur vacancy on the sulfide surface. The observed zero-order in S_2 for S-ZrO_2 signifies that gas phase sulfur is involved after the rate-determining step. Thus, akin to the mechanism of traditional ODHP, the role of gas phase sulfur (S_2) would be to replenish the surface sulfur vacancies.

As the M-S bond becomes increasingly weak, the surface reduction by propane could become more facile to the extent that re-sulfidation of the surface becomes the slower step. The point at which re-sulfidation becomes rate-determining may conceivably correspond to the peak of the "volcano" trend in Figure 8. This explanation plausibly accounts for the higher E_{app} and observed half-order in sulfur for S-Co_3O_4. Additionally, the presence of Co^0 on the surface of S-Co_3O_4 as discussed above suggests that this catalyst is easily reduced and less easily sulfided compared to other SODHP catalysts. Note that, although sulfur vapor is preheated to 700 °C prior to reaction with propane (see Experimental Section), the actual SODHP reaction temperature is 550 °C or lower. Thus, it is possible that other sulfur allotropes such as S_8 or S_7 may be present in the reactant stream.[9-11] Future experimental and theoretical work will be needed to characterize the nature of the sulfur vapor oxidant in more detail.

Conclusions

This investigation aimed to expand the previous S_2 "soft oxidant" approach as an OCM analogue to an ODHP analogue and to explore the activity of metal sulfide catalysts in this reaction. The data presented here, including catalyst characterization and reactivity studies, are summarized in Table 1. Gaseous elemental sulfur is found to be an effective oxidant for ODHP, and the product selectivities vary significantly depending on the metal sulfide catalyst identity (86% propylene over S-ZrO_2 versus 38% over PdS at 550 °C, for example). The experimental E_{app} values for propylene formation are shown to scale/increase with increasing XPS sulfur binding energy, a qualitative experimental estimate of M-S bond strength and electron density. This result, combined with reaction orders of C_3H_8 and S_2, suggest a mechanism in which surface sulfur species initiate C-H activation and gas phase S_2 replenishes the vacancies resulting from product formation. Additionally, respectable propylene yields are obtained for a number of the catalysts examined. The findings reported in this study demonstrate that SODHP is a viable route to selective propylene formation over inexpensive and sulfur-tolerant catalysts. Further experimental and theoretical studies of SODHP catalyst development are ongoing.

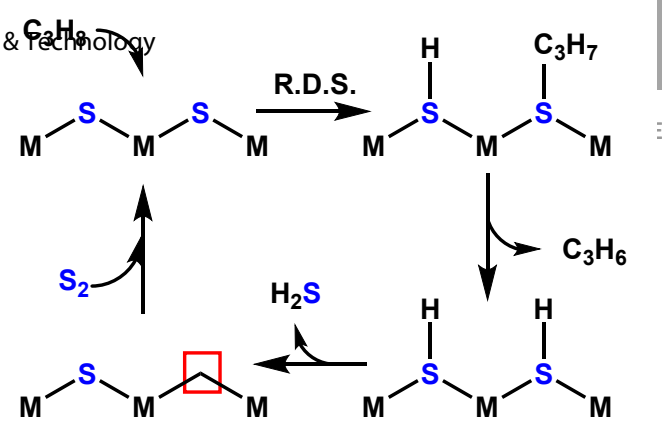

Figure 10. Proposed mechanism for SODHP over metal sulfide catalysts. The red box represents a sulfur vacancy, M is the metal of a given metal sulfide, and R.D.S. stands for the rate-determining step.

Conflicts of interest

There are no conflicts to declare.

Acknowledgements

We thank the Center for Innovative and Strategic Transformation of Alkane Resources (CISTAR, NSF award number 1647722) for supporting this project. The authors acknowledge Prof. Justin Notestein for helpful discussions and Dr. Neil Schweitzer for use of the Northwestern Reactor Engineering and Catalysis Testing (REACT) facility. This work made use of the Jerome B. Cohen X-Ray Diffraction Facility supported by the MRSEC program of the National Science Foundation (DMR-1720139) at the Materials Research Center of Northwestern University and the Soft and Hybrid Nanotechnology Experimental (SHyNE) Resource (NSF ECCS-1542205). This work made use of the Keck-II facility of Northwestern University's NU*ANCE* Center, which has received support from the Soft and Hybrid Nanotechnology Experimental (SHyNE) Resource (NSF ECCS-1542205); the MRSEC program (NSF DMR-1720139) at the Materials Research Center; the International Institute for Nanotechnology (IIN); the Keck Foundation; and the State of Illinois, through the IIN.

References

1 National Academies of Sciences, Engineering, and Medicine, The Changing Landscape of Hydrocarbon Feedstocks for Chemical Production: Implications for Catalysis: Proceedings of a Workshop, The National Academies Press, Washington, DC, 2016.
2 J. J. H. B. Sattler, J. Ruiz-Martinez, E. Santillan-Jimenez and B. M. Weckhuysen, *Chem. Rev.*, 2014, **114**, 10613-10653.
3 F. Cavani, N. Ballarini and A. Cericola, *Catal. Today*, 2007, **127**, 113-131.
4 T. Ren, M. Patel and K. Blok, *Energy*, 2006, **31**, 425-451.
5 C. A. Carrero, R. Schloegl, I. E. Wachs and R. Schomaecker, *ACS Catal.*, 2014, **4**, 3357-3380.
6 Q. Zhu, S. L. Wegener, C. Xie, O. Uche, M. Neurock and T. J. Marks, *Nat. Chem.*, 2013, **5**, 104-109.
7 M. Peter and T. J. Marks, *J. Am. Chem. Soc.*, 2015, **137**, 15234-15240.
8 S. Liu, S. Udyavara, A. Arinaga, M. Neurock and T. J. Marks, presented in part at ACS Spring 2020 National Meeting and Expo, Philadelphia, PA, 2020. https://doi.org/10.1021/scimeetings.0c01381
9 B. Meyer, *Chem. Rev.*, 1976, **76**, 367-388.

10 H. Rau, T. R. N. Kutty and J. R. F. Guedes De Carvalho, *J. Chem. Thermodyn.*, 1973, **5**, 833-844.
11 A. J. Jackson, D. Tiana and A. Walsh, *Chem. Sci.*, 2016, **7**, 1082-1092.
12 E. Cheng, L. McCullough, H. Noh, O. Farha, J. Hupp and J. Notestein, *Ind. Eng. Chem. Res.*, 2020, **59**, 1113-1122.
13 G. Wang, C. Gao, X. Zhu, Y. Sun, C. Li and H. Shan, *ChemCatChem*, 2014, **6**, 2305-2314.
14 G. Wang, C. Li and H. Shan, *ACS Catal.*, 2014, **4**, 1139-1143.
15 G. Wang, N. Sun, C. Gao, X. Zhu, Y. Sun, C. Li and H. Shan, *Appl. Catal., A*, 2014, **478**, 71-80.
16 R. Watanabe, N. Hirata, K. Miura, Y. Yoda, Y. Fushimi and C. Fukuhara, *Appl. Catal., A*, 2019, **587**, 117238.
17 M. M. Johnson and H. J. Hepp, *US Pat.,* US3280210A, 1966.
18 P. E. Højlund-Nielsen, R. M. Nielsen, and L. J. Lemus-Yegres, WO Pat., WO2017162427A1, 2017.
19 J. R. Rostrup-Nielsen, presented in Progress in Catalyst Deactivation, Dordrecht, 1982.
20 J. A. Rodriguez and J. Hrbek, *Acc. Chem. Res.*, 1999, **32**, 719-728.
21 A. D. Cohen, *US Pat.,* US3456026A, 1969.
22 L. J. Croce and L. Bajars, *US Pat.,* US3666687A, 1972.
23 L. J. Croce and L. Bajars, *US Pat.,* US3937746A, 1976.
24 V. Mohan and I. S. Pasternak, *US Pat.,* US3403192A, 1968.
25 I. S. Pasternak, A. D. Cohen, and N. J. Gaspar, *US Pat.,* US3585250A, 1971.
26 Z. A. Premji, J. M. H. Lo and P. D. Clark, *J. Phys. Chem. A*, 2014, **118**, 1541-1556.
27 P. D. Clark, N. I. Dowling, X. Long and Y. Li, *J. Sulfur Chem.*, 2004, **25**, 381-387.
28 E. Jüngst and W. Nehb, Wiley-VCH, Weinheim, 2008, Ch. Chapter 12.4.
29 W. Luc and F. Jiao, *Acc. Chem. Res.*, 2016, **49**, 1351-1358.
30 M. Zhang, Y. Zhu, X. Wang, Q. Feng, S. Qiao, W. Wen, Y. Chen, M. Cui, J. Zhang, C. Cai and L. Xie, *J. Am. Chem. Soc.*, 2015, **137**, 7051-7054.
31 NIST *X-ray Photoelectron Spectroscopy Database*, https://srdata.nist.gov/xps/ (accessed May 2020).
32 K. Fukudome, N.-o. Ikenaga, T. Miyake and T. Suzuki, *Catal. Sci. Technol.*, 2011, **1**, 987-998.
33 K. Chen, E. Iglesia and A. T. Bell, *J. Phys. Chem. B*, 2001, **105**, 646-653.
34 X. Sun, Y. Ding, B. Zhang, R. Huang and D. S. Su, *Chem. Commun.*, 2015, **51**, 9145-9148.
35 C. Carrero, M. Kauer, A. Dinse, T. Wolfram, N. Hamilton, A. Trunschke, R. Schlögl and R. Schomäcker, *Catal. Sci. Technol.*, 2014, **4**, 786-794.
36 E. V. Kondratenko, M. Cherian, M. Baerns, D. Su, R. Schlögl, X. Wang and I. E. Wachs, *J. Catal.*, 2005, **234**, 131-142.
37 J. T. Grant, C. A. Carrero, A. M. Love, R. Verel and I. Hermans, *ACS Catal.*, 2015, **5**, 5787-5793.
38 E. V. Kondratenko, M. Cherian and M. Baerns, *Catal. Today*, 2005, **99**, 59-67.
39 S. Dahl, A. Logadottir, C. J. H. Jacobsen and J. K. Nørskov, *Appl. Catal. A*, 2001, **222**, 19-29.
40 J. A. Dumesic, G. W. Huber and M. Boudart, *Principles of Heterogeneous Catalysis*, In *Handbook of Heterogeneous Catalysis*, 2008.
41 K. Chen, A. Khodakov, J. Yang, A. T. Bell and E. Iglesia, *J. Catal.*, 1999, **186**, 325-333.
42 K. Routray, K. R. S. K. Reddy and G. Deo, *Appl. Catal., A*, 2004, **265**, 103-113.
43 D. Creaser, B. Andersson, R. R. Hudgins and P. L. Silveston, *J. Catal.*, 1999, **182**, 264-269.
44 K. Chen, A. T. Bell and E. Iglesia, *J. Phys. Chem. B*, 2000, **104**, 1292-1299.
45 R. R. Chianelli, *Catal. Rev.*, 1984, **26**, 361-393.
46 K. Murata, D. Kosuge, J. Ohyama, Y. Mahara, Y. Yamamoto, S. Arai and A. Satsuma, *ACS Catal.*, 2020, **10**, 1381-1387.
47 M. Badlani and I. E. Wachs, *Catal. Lett.*, 2001, **75**, 137-149.
48 A. Burri, N. Jiang, K. Yahyaoui and S.-E. Park, *Appl. Catal., A*, 2015, **495**, 192-199.
49 A. J. Medford, A. Vojvodic, J. S. Hummelshøj, J. Voss, F. Abild-Pedersen, F. Studt, T. Bligaard, A. Nilsson and J. K. Nørskov, *J. Catal.*, 2015, **328**, 36-42.
50 D. Kiani, S. Sourav, W. Taifan, M. Calatayud, F. Tielens, I. E. Wachs and J. Baltrusaitis, *ACS Catal.*, 2020, **10**, 4580-4592.
51 K. Chen, E. Iglesia and A. T. Bell, *J. Catal.*, 2000, **192**, 197-203.
52 B. Mitra, I. E. Wachs and G. Deo, *J. Catal.*, 2006, **240**, 151-159.

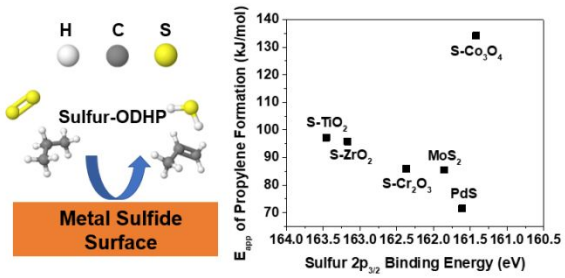

Sulfur vapor (S_2) is explored as a “soft” oxidant for the selective catalytic dehydrogenation of propane to propylene over a variety of metal sulfide surfaces.